Volume 12
Number 16
21 August 2024
Pages 3973-4264

Biomaterials Science

rsc.li/biomaterials-science

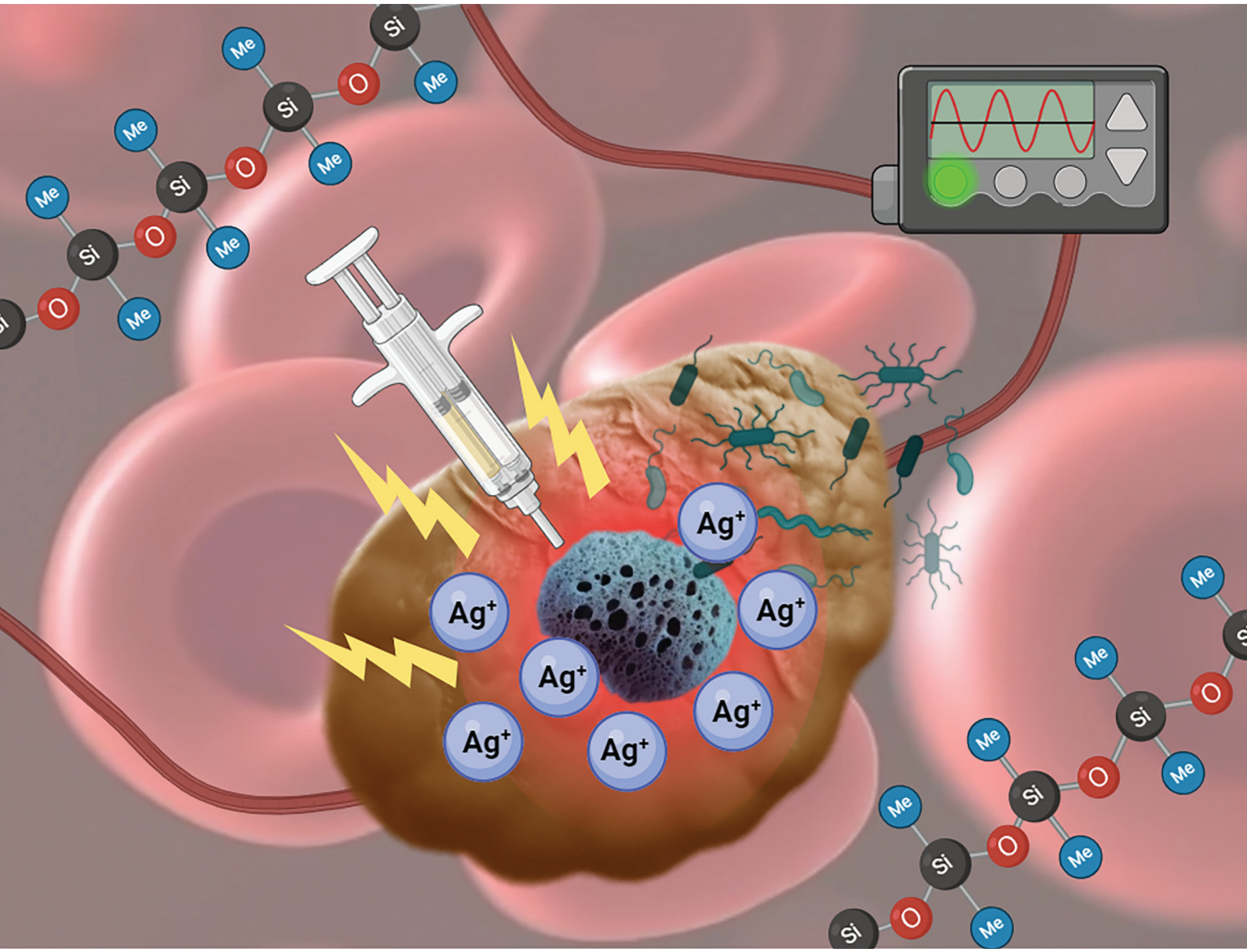

ISSN 2047-4849

ROYAL SOCIETY OF CHEMISTRY

PAPER
Kausik Mukhopadhyay *et al.*
Antibacterial sponge for rapid noncompressible hemostatic treatment: spatiotemporal studies using a noninvasive model

European Society for Biomaterials

Biomaterials Science

ROYAL SOCIETY OF CHEMISTRY

PAPER

View Article Online
View Journal | View Issue

Cite this: *Biomater. Sci.*, 2024, **12**, 4155

Antibacterial sponge for rapid noncompressible hemostatic treatment: spatiotemporal studies using a noninvasive model†

Pritha Sarkar,[a] Abinaya Sindu Pugazhendhi,[b] Melanie Coathup[b] and Kausik Mukhopadhyay *[a]

Hemorrhage is one of the leading causes of preventable death. While minor injuries can be treated mainly by conventional methods, deep and irregular wounds with profuse bleeding present significant challenges, some of which can be life-threatening and fatal. This underscores the need to develop easily applicable FDA-approved hemostatic treatments that can effectively stanch blood loss at the point of care before professional medical care. A silicone-based bandage system (SilFoam), a non-compressible, self-expanding, antibacterial hemostatic treatment, is reported here. Its two-component system reacts *in situ* upon mixing to form a stretchable sponge that acts as a 'tamponade' by expanding within seconds with the evolution of oxygen gas from the interaction of the reactive components present in the formulation. This generates autogenous pressure on the wound that can effectively arrest heavy bleeding within minutes. Possessing optimal adhesive properties, the expanded sponge can be easily removed, rendering it optimal for hemostatic wound dressing. With recent advances in biotechnological research, there is a growing awareness of the potential issues associated with *in vivo* trials, spanning ethical, psychological, economic, and physiological concerns like burnout and fatigue. Bearing this in mind, a unique manikin system simulating a deep abdominal wound has been employed to investigate SilFoam's hemostatic efficacy with different blood-flow rates using a non-invasive model that aims to provide an easy, fast, and economical route to test hemostatic treatments before *in vivo* studies. This is the first time an Ag_2O-based oxygen-induced foaming system has been reported as a hemostatic agent.

Received 12th April 2024,
Accepted 19th June 2024

DOI: 10.1039/d4bm00506f

rsc.li/biomaterials-science

1. Introduction

Hemorrhage and uncontrollable blood loss remain the primary causes of preventable death for civilians and soldiers on the battlefield.[1–4] In a study on combat casualties in 2012, it was found that noncompressible hemorrhage was responsible for most of the military deaths investigated.[5] Further analysis of the data collected revealed that almost all fatalities from hemorrhage occurred before arriving at a medical facility. Another article from 2019 emphasized how traumatic injuries and hemorrhage remain the leading causes of death, with severe bleeding accounting for around 40% of deaths even outside military conflict.[6] Most homicide deaths occur due to nonsurvivable injuries, of which traffic accidents and violence contribute to high rates of fatal hemorrhages.[7] While a patient with blunt trauma has an hour of 'golden time' before adopting appropriate therapy, patients with penetrating trauma only have a 'platinum five minutes' during which catastrophic hemorrhage may still occur.[6–8] Controlling bleeding and extending the prehospital interval may, therefore, literally mean the difference between life and death, and quick action is essential to enhancing survival prospects. This undeniable need has spearheaded a surge in hemostatic research, which has led to a plethora of diverse and successful hemostats – both synthetic and natural, many of which have also been translated to commercial technology such as Quikclot®, CELOX®, Hemcon®, Surgicel®, *etc.*[8–11] Unfortunately, the perfect hemostatic dressing still does not exist. Ideally, the dressing should be lightweight, easy to store, and able to be rapidly applied to a hemorrhaging wound without getting washed away. It should be conformable in and around the wound, allowing the hemostatic agent to reach areas of injury that are difficult to access with direct pressure (*i.e.*, deep groin wounds). The dressing should cause minimal local tissue destruction and not contain particles that can spread around

[a]*Department of Materials Science and Engineering, University of Central Florida, Orlando, USA. E-mail: kausik@ucf.edu*
[b]*Biionix Cluster and College of Medicine, University of Central Florida, Orlando, USA*

† Electronic supplementary information (ESI) available. See DOI: https://doi.org/10.1039/d4bm00506f

the wound and body systemically.[10,11] Further, such materials and devices must be readily applicable in times of crisis. It should be considered that in a state of shock, panic can cause the administration of intravenous treatments or other complex operations to be complicated. Bandages and topical treatments are popular and easy to administer in such situations. However, bandage systems such as gauze and tourniquets have gained inadequate success regarding sterility, pressure, and adhesion.[11,12] These issues have been challenged by novel bandage systems and topical treatments such as foams, gels, creams, powders, nanofibers, *etc*.[9,13–18] Many of these inventions have produced excellent results *in vitro* and *in vivo*, but their mechanical properties are seldom extensively studied. The success of a hemostat on a calm and stationary subject can be very different from that of an active person. It should be mechanically sound, able to sustain friction and torsion from moving muscles, and should not slip off the wound easily. There is, hence, a need to evaluate the mechanical properties of hemostats and their performance *in vitro* and *in vivo*. Currently, one of the commonly used treatments is QuikClot®. However, it has been reported that it has limited efficacy for high-pressure bleeding wounds since the powder granules tend to get washed away by the bleeding before they can form clots.[1,19] Further, the dressing generates heat in interaction with blood, which is a potential cause for burns.[1,20] Another common combat hemostat is Celox®, a chitosan-based powder hemostat. Although no heat is involved, it is weak against high-pressure bleeding, and some reports mention that small insoluble chitosan particles can enter the bloodstream and get transported to small blood vessels, causing distant normal blood vessel embolism.[19,21,22] Another recent market dressing is GelFoam®, a compressed sponge made from porcine skin gelatin. These foams are theoretically bio-resorbable; however, if left near tissue or bone, it has been found that they may induce fibrosis and necrosis.[23,24] Recent research on developing novel hemostatic materials has largely focused on applying surgical sealants and adhesives, where biodegradability plays an important role. They are often expensive, sensitive, and require careful application, hence unsuitable for field operations and emergencies.[9] Hydrogels and sponges gained popularity due to their excellent blood absorption qualities. In addition, there is plenty of scope to load them with bioactive substances such as antibiotics and painkillers.[15,25–28] Sponges have suitable texture and mechanical properties for a dressing material.[8,29–31] There has been considerable research and success in developing hemostatic sponges based on natural and synthetic materials.[29,32–36] In a previous study by Choudhary *et al.*, an injectable two-part foam system based on chitosan and alginate has been developed,[37] which employs CO_2 as a blowing agent. The prospect of self-expanding foams for hemostasis has also been explored with the self-expanding polyurethane foam known as ResQFoam®. When subcutaneously injected into the abdominal cavity, this foam can expand, effectively providing volume-filling to impede bleeding. However, concerns regarding thermal injuries and bowel injuries have been raised, resulting in potential risks about its use.[10,38] Another similar injectable expandable system, XStat®, is available on the market and has been investigated in this study.

In the current study, these concerns have been carefully considered. Here, a rapid-action PDMS-Ag_2O-based antimicrobial hemostatic sponge bandage system, SilFoam, capable of withstanding uncompromising blood loss, has been developed. One of the primary objectives was to create an O_2-based foaming system while avoiding using naturally derived substances due to problems associated with storage and the possibility of unwanted interactions in the body. The two-component mixture of this hemostatic system chemically reacts to form a stiff, non-toxic sponge that develops an artificial blockage, creating autogenous pressure on the wound to control and arrest profuse bleeding. The other focus of the study was to facilitate an animal-free testing procedure for comparing SilFoam and other hemostatic bandage systems. In light of this, a simplistic solution that does not involve *in vivo* protocols has been explored: using a mechanical hemorrhage model – a manikin- to test the hemostatic efficacy of SilFoam noninvasively. A dual syringe system makes administration and storage of SilFoam hassle-free, and the resultant sponge formed upon the interaction of the two-part formulation acts as a tamponade by expanding rapidly, conforming on and around the site of injury to control profuse bleeding within seconds. Based on modular studies, the sponge can be removed without any form of tissue damage. This study has been focused on evaluating the biocompatibility and mechanical properties of the hemostatic sponge to determine if its robustness and adhesive properties are conducive to performance in combat settings (hydrophobicity, reaction time, ease of application, ease of storage, durability, *etc*.). SilFoam aims to provide the injured party with a means to rapidly stagnate or arrest bleeding from external and internal wounds in a manner superior to those currently available. It presents a simple and economical approach to a biocompatible hemostatic bandage system with spontaneous self-expanding properties that can remain functional under inclement weather conditions.

2. Methods

2.1. Materials

Commercial polydimethylsiloxane(PDMS) part A and part B, platinum-divinyltetramethyldisiloxane complex (Pt-PDMS, Gelest Inc., Morrisville, PA, USA), silver(I) oxide powder (Ag_2O), hydrogen peroxide (30% H_2O_2 in H_2O) and Phosphate Buffered Saline 1× (PBS, ThermoScientific Co., Waltham, MA, USA), fumed silica (Evonik Co., Essen, Germany), polysorbate 80 (Tween80, Fisher Bioreagents Co., Hampton, NH, USA), artificial blood (same viscosity as human blood ~4.5 cP VATA Inc., Canby, OR, USA), *Escherichia coli (E. coli)* and *Staphylococcus aureus* (*S. aureus*; ATCC, Manassas, VA, USA), Luria–Bertani (LB) broth and Agar (Sigma Aldrich, St Louis, MO, USA); Celox® gauze, HemCon Chitogauze®, XStat®, and Everlit®

Alginate Dressing were procured and investigated in this study. Dual syringe devices were procured from Ellsworth Adhesives (Germantown, WI, USA). Pig skin and sausage skin (collagen casings) were procured from the local supermarket (Super Oriental Market, Orlando, FL.).

2.2. Procedure

Precursors for SilFoam – parts A and B were prepared separately. 8.5 g of PDMS-A was added to a speed mixer cup to prepare part A. Tween80 was added, followed by 0.176 g of Pt-PDMS being added dropwise. 0.4 g of Ag_2O was then added to the mixture. Before this, varying amounts of Ag_2O were attempted to optimize the weight (ESI Fig. S1†). The cup was loaded into the FlackTek (Landrum, South Carolina, USA) speed mixer. After mixing for 40 seconds at 2400 rpm, the cup was removed and kept aside. Similarly, 8.5 g of PDMS B was added to a speed mixer cup to prepare part B. Tween80 was added, followed by fumed silica. 1.7 g of 30% H_2O_2 was then added dropwise to this mixture. The cup was then loaded into the FlackTek speed mixer. After mixing for 40 seconds at 2000 rpm, the cup was removed and kept aside. The compositions of part A and part B are shown in ESI Table 1.† For delivery, 10 mL of part A and 10 mL of part B were loaded into separate compartments of a dual syringe device. A polypropylene turbulator was attached to the opening for mixing on delivery (Fig. 2b). The mixture was then pumped out for expansion, temperature, and rheology studies.

2.3. Surface morphology

The cellular structure of the SilFoam sponges was observed by scanning electron microscopy (JEOL JSM-6480 SEM (Tokyo, Japan)) at an acceleration voltage of 10 kV. Energy-dispersive X-ray spectroscopy (EDS) and elemental analysis were performed to quantify relative amounts of Ag, Si, and O on the surface. The pore size distribution and average size of the pores on the sponge surfaces were analyzed using ImageJ software.

2.4. Temperature and expansion

Temperature and expansion studies were performed to study and optimize the heat generated during the exothermic reaction, along with the volume expansion of SilFoam on mixing. An IR temperature gun (Fotric 348A (Dallas, Texas, USA)) was used for temperature studies. 5 mL of the respective samples were delivered from the dual syringe devices into graduated falcon tubes. The temperature gun was then used to record the temperature with volume expansion, and the highest temperature was noted along with the maximum expansion height. A companion software (Analyzr) was used to analyze the live temperature profiles during the expansion process.

2.5. Rheology

Rheological tests were performed to assess the viscosity, flowability, storage, and loss moduli of SilFoam. Rheology experiments were performed with the TA Instruments HR20 rheometer. A pea-sized sample was delivered onto a 25 mm steel Peltier plate using a dual syringe. Viscosity measurements were taken with a flow sweep shear test from 1 per second to 100 per second at room temperature (25 °C). For gel-to-foam testing, a disk of pig skin was cut and attached to the Peltier plate to simulate contact with skin. A time sweep test was performed at room temperature at a constant strain of 0.2% and frequency of 1 Hz for 15 minutes, followed by an axial test to study the tack. The axial test was conducted at a head velocity of 10 μm per second. The same experiment was then performed with an immersion cup filled with PBS to study the rheological behavior in an aqueous environment to simulate blood.

2.6. Dynamic mechanical analysis (DMA)

DMA tests were carried out to quantify the storage modulus of cured SilFoam. A DMA test in compression mode was carried out with the TA Instruments HR20 rheometer (New Castle, Delaware, USA). Cured SilFoam was cut into a disk with a diameter of 25 mm and 5 mm thick. The test was run at room temperature (25 °C) at a frequency of 1 Hz. A linear sweep was carried out from an axial displacement of 1 μm to 100 μm at increments of 5 μm.

2.7. Compression testing

The compressive stress–strain measurements were performed using a tensile-compressive tester (Shimadzu Universal Testing Machine AGS-X (Kyoto, Japan) with a 1 kN sensor). In a typical test, cured SilFoam samples were cut in cylindrical shapes (25 mm in diameter and 10 mm in depth), and the compressive strain rate was set to 5 mm min^{-1}. The compressive modulus was the approximate linear fitting value of the stress–strain curves in the 15–25% strain range.

2.8. Lap shear testing

The lap shear test was performed according to a previous study.[25] The lap shear strength of SilFoam was tested according to the modified ASTM F2255-05 standard for the lap shear strength property of tissue adhesives. The sausage skin membrane was bonded to two glass slides with cyanoacrylate glue. Then, 1 mL of the SilFoam mixture was injected on the membrane surface of a glass slide (20 mm × 25 mm) *via* a dual syringe, as shown above. Finally, another glass slide was bonded to it (20 mm × 25 mm) with cyanoacrylate glue. The two glass slides were placed into a Shimadzu Universal Testing Machine AGS-X for shear testing by tensile loading with a strain rate of 1 mm per minute (ESI Fig. S5†). The shear strength was determined at the point of detachment.

2.9. Attenuated total reflection-Fourier transform infrared spectroscopy (ATR-FTIR)

The PerkinElmer FT-IR Spectrometer Spectrum 3 (Waltham, Massachusetts, USA) and the Fast Scan accessory were used to analyze the FTIR spectra transition of reacting SilFoam in real-time in ATR mode. An MCT (Mercury Cadmium Telluride) detector was used with a diamond crystal for ATR. The fast

scan was performed at 16 accumulations per minute in the wavenumber range of 650 cm^{-1} to 4000 cm^{-1} for 5 minutes. Part B was first loaded onto the detector plate, followed by adding and mixing part A after 30 seconds. Prior to this, the normal spectra of SilFoam part A and SilFoam part B were taken individually for reference (ESI Fig. S6†).

2.10. Inductively coupled plasma optical emission spectroscopy (ICP-OES)

The ICP-OES investigation was conducted with a PerkinElmer Avio 500 Max (Waltham, Massachusetts, USA). 0.1 g of cured SilFoam was left to soak in 4 g of PBS solution for 1 hour and 24 hours, respectively. The SilFoam was removed, and ICP-OES analysis was performed to determine the concentration of silver ions in the solutions. Before inspection, the solutions were diluted to a total volume of 50 mL. The solutions were then acidified with 5 mL of HNO_3 to make the final acid concentration 10%. The prepared samples were nebulized, and the resulting aerosol was transferred to the plasma torch, which used radio frequency inductive coupling plasma to generate the elements' spectra. The spectra were dispersed using a grating spectrometer, and the intensity of emission lines was monitored using a photosensitive detector. The Quantitation Limit Verification was 0.02 mg L^{-1}, and the calibration range was from 0.0–0.5 mg L^{-1}.

2.11. Hydrophobicity

The Krüss Drop Shape Analyzer DSA25 (Hamburg, Germany) contact angle goniometer was used to study the surface contact angle of the hemostatic sponges. Static contact angles were measured using a 0.2 mm needle to disperse 4 μL of deionized (DI) water onto the SilFoam sponge surface at a 2 μl per second rate.

2.12. Thermogravimetric analysis

Thermogravimetric analysis of SilFoam was conducted using PerkinElmer STA 6000 equipment (Waltham, Massachusetts, USA). A small portion of cured SilFoam was weighed and loaded in a ceramic pan for testing. The sample was heated at 20 °C per minute from 30 °C to 500 °C in an inert N_2 gas atmosphere at a 20 mL per minute flow rate.

2.13. Swelling test

A swelling test was performed to test the fluid absorption capacity of SilFoam and commercial hemostatic materials – Celox® gauze, Hemcon Chitogauze®, XStat®, and Everlit® Alginate Dressing. A small amount of each sample was weighed and allowed to soak in a beaker filled with artificial blood for 10 minutes. Afterward, the wet samples were removed, wiped gently with absorbent wipes to clear excess fluid on the surface, and weighed again. The absorption capability was calculated as –

$$\text{Absorption by weight}(\%) = \frac{\text{Wet weight} - \text{Dry weight}}{\text{Dry weight}} \times 100$$

2.14. Mechanistic hemorrhage manikin model

A silicone manikin provided by SIMETRI, Inc. (Orlando, Florida, USA) simulating a deep torso hemorrhage wound was used to determine the hemostatic capability of SilFoam. The manikin depicts a realistic annular wound roughly 2 cm wide and 4 cm long, fed through a fluid supply (ESI Fig. S4†). When switched on, the manikin was connected to an electronic bleeding controller, which supplies fluid to the open wound at a flow rate of 0.5 mL per second. A tablet was used to communicate with the bleeding controller *via* a Bluetooth connection. Artificial blood (the same viscosity as blood) was used to experiment to simulate natural conditions better. Bleeding was activated, the SilFoam mixture was injected immediately on the wound site, and time to leakage was noted. The same procedure was repeated with commercial hemostatic agents – Celox® gauze, Chitogauze®, XStat®, and Everlit® Alginate dressing for a comparison study with SilFoam, both with and without wound packing.

2.15. Minimal essential media (MEM) elution test

MEM Elution tests were conducted with 0.2 g mL^{-1} extraction ratios with cured SilFoam. Test articles and controls were extracted in 1× Minimal Essential Media with 5% bovine serum for 24 hours at 37 °C with agitation. Multiple-well cell culture plates were seeded with a verified quantity of industry-standard L-929 cells (ATCC CCL-1) and incubated until approximately 80% confluent. The test extracts were held at room temperature for less than four hours before testing. The extract fluids were not filtered, centrifuged, or manipulated in any way following the extraction process. The test extracts were added to the cell monolayers in triplicate. The cells were incubated at 37 °C for 48 hours. Polypropylene pellets were used as a negative control, and latex natural rubber was used as a positive control.

2.16. MTT assays

MTT assays were performed using mouse CCL-NCTC clone 929 cells (L929) obtained from ATCC. Cell culture plates (96-well) were seeded and incubated until approximately 50% confluent. The amount of material extracted was based on ISO surface area or weight recommendations. Test articles and controls were extracted under agitation in 1× Minimal Essential Media with 5% bovine serum (1×MEM5) at 37 °C. The following dilutions were tested: diluted 2-fold (50%), diluted 4-fold (25%), and diluted 8-fold (12.5%). The test article and control extracts were exposed to the cells by adding 100 μL to each of the six wells in the 96-well plate. The media control was exposed to the cells by adding 100 μL to each of the 12 wells. The top and bottom rows were not seeded with cells and served as the test system blank. The blank wells each received 100 μL aliquots of 1×MEM5. The plate was then incubated at 37 °C in humidified conditions for 24 hours. The extracted fluid was removed from the plate, and 50 μL of a 1 mg mL^{-1} MTT solution was added to each well of the plate. The plate was then incubated for 2 hours before removing the MTT solu-

tion from the wells. 100 μL of isopropanol was added to each well of the plate to extract the metabolized MTT from the viable cells. The plate was covered and placed on an orbital shaker at 120 RPM for 1 hour. The absorbance at 570 nm was measured on a spectrophotometer with a reference wavelength of 650 nm. Percent viability was calculated as follows, where OD = optical density:

$$\text{Percent viability} = \frac{\text{Mean Test Article OD}}{\text{Mean Media Control OD}} \times 100\%$$

2.17. Hemolysis

The hemolytic index of SilFoam was analyzed following ASTM F 756. An equal amount of blood from 3 donors was drawn into vacutainers containing 0.1 M sodium citrate at a ratio of 9 : 1 (3.2% anticoagulant to blood). A hemoglobin standard was diluted with Drabkin's reagent to give solutions at concentrations of 0.80, 0.60, 0.40, 0.30, 0.20, 0.10, 0.02, and 0.01 mg mL^{-1}. The absorbance was read on a spectrophotometer at 540 nm. A standard curve was determined using linear regression with the absorbance values and the standard concentrations of hemoglobin. The blood was centrifuged, and the plasma-free hemoglobin concentration was determined. The total amount of hemoglobin present was determined by adding a 20 μL aliquot of the blood to 5 mL of Drabkin's reagent and measuring the absorbance at 540 nm. The hemoglobin concentration was determined from the standard curve, and dilution was accounted for. SilFoam was incubated in PBS at 37 °C for 24 hours, using an extraction ratio of 0.2 g mL^{-1}. A non-hemolytic negative control, a hemolytic positive control, and a PBS blank were included and extracted at the same time and temperature as SilFoam. Three of each control and the PBS blank were prepared in test tubes. To each test tube, 7 mL of each SilFoam extract, control, or PBS blank extract, and 1 mL of diluted blood was added. The tubes were then incubated at 37 °C for 3 hours. The tubes were gently inverted twice at 30 minute intervals throughout the incubation period. After incubation, the test articles and controls were centrifuged, and 1 mL of the supernatant fluid was combined with 1 mL of Drabkin's reagent. The test articles and controls were then read at 540 nm in a spectrophotometer. The hemolytic index was interpreted from the following equation:

$$\text{Hemolytic index}(\%) = \frac{\text{Hemoglobin released}(\text{mg mL}^{-1})}{\text{Hemoglobin present}(\text{mg mL}^{-1})} \times 100$$

The corrected hemolytic index was calculated by subtracting the hemolytic index of the PBS blank solution from the hemolytic index of SilFoam and the controls.

2.18. Antibacterial assays

The antimicrobial efficiency of SilFoam was evaluated using the disc diffusion method against *S. aureus* ATCC 6538 (Gram-positive) and *E. coli* ATCC 43888 (Gram-negative). All samples were cut into 8 mm diameter disks and sterilized by UV radiation for 15 minutes, exposing both sides of the sample. The SilFoam disks were placed onto an agar plate surface containing a nonselective medium, Laria Bertani agar (LBA). The agar plates were inoculated separately with a suspension of *S. aureus* and *E. coli* of ~10^5 CFU mL^{-1} in 0.7% overlay agar to give a confluent lawn of growth. PDMS disks were used as controls. Interpretative inhibition zone diameters have been established for susceptibility test results. Interpretation of susceptibility and resistance to samples was based only on the presence or absence of a zone of inhibition (mm) surrounding the disc following 16 hours of incubation. For the growth curves, *S. aureus* and *E. coli* (~10^6 CFU ml^{-1}) were co-incubated with a dispersion of the working concentration of silver oxide (positive control), PDMS (negative control), and SilFoam (disks: diameter: 8 mm, thickness: 1 mm) to evaluate their antibacterial activity at 37 °C for 24 h at 210 rpm. At different time points (0, 4, 8, 12, 16, 20, and 24 h), the bacterial suspension was withdrawn and spread onto an agar plate. After 24 h incubation, the colony-forming units were measured. All experiments were carried out in triplicates.

2.19. Statistical analysis

Experiments were conducted with a minimum of triplicate sets of data. Data were represented as mean ± SD (standard deviation of the mean value) unless indicated otherwise and compared by a two-tailed Student's *T*-test. Differences were considered statistically significant when the *p*-value was <0.05. Statistical significance is indicated by ns $p > 0.05$, $*p < 0.05$, $**p < 0.01$, $***p < 0.001$, and $****p < 0.0001$.

3. Results and discussion

3.1. Temperature and expansion

The SilFoam foam was fabricated by silicone curing aided by a Pt-based curing catalyst. PDMS-A in part A comprises vinyl-terminated silicone oligomers, and PDMS-B in part B comprises functional silicone crosslinkers. Rapid curing occurs when mixed in a 1 : 1 ratio in the presence of a Pt-catalyst, resulting in a crosslinked solid PDMS network. The position and concentration of both vinyl (–CH=CH_2) and hydride (–Si–H) groups along the siloxane backbone decide the nature of the elastomeric network.[39] An important signature during the crosslinking is the so-called gel point. It characterizes the state when a 3-dimensional network of crosslinked molecules is formed.[40] Therefore, it transitions from a viscoelastic liquid to a viscoelastic solid.[39,41,42] In this case, the curing process is further accelerated by the heat of the decomposition of H_2O_2. Peroxides are known to be effective oxygen generators in materials engineering, including materials for biomedical applications.[43,44] The decomposition of H_2O_2 is an exothermic process. Ag_2O works as a catalyst when the hydrogen peroxide-containing part B comes into contact with part A, initiating the reaction $H_2O_2 \rightarrow H_2O + O_2$, which breaks down hydrogen peroxide into oxygen and water.[45,46] A simplified scheme is shown in Fig. 1. The heat of the reaction serves two purposes – firstly, it helps speed up the polymerization process and, hence, the formation of the sponge; secondly, it lowers the vis-

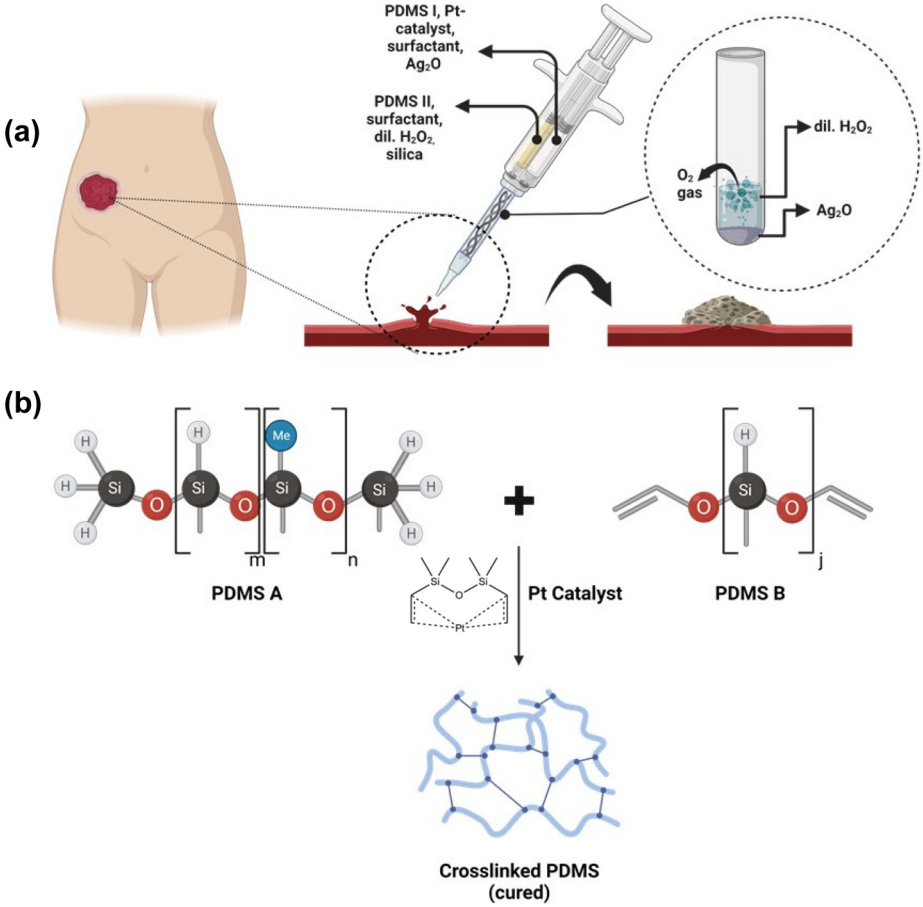

Fig. 1 Schematic illustration of SilFoam fabrication (a) methodology and application; (b) PDMS curing process.

cosity of part B, facilitating easier delivery. However, too much heat is undesirable as it poses the risks of burns and necrosis. It has been seen that temperatures as low as 44 °C can cause tissue damage.[47] Hence, it was important to ensure that the system's temperature remained below 35 °C (95°F), even at the expense of lower expansion. Different weights of silver oxide were tested to optimize the expansion/temperature and obtain the formulation that shows maximum expansion within the stipulated safe temperature maximum (ESI Table S1†). It was concluded that 2 wt% of Ag_2O would be most suitable for subsequent formulations because it showed the highest volume expansion within safe temperatures (ESI Fig. S1†). SilFoam was therefore prepared with 2 wt% Ag_2O, as described in the Experimental section above. A 5× volume expansion was observed in 30 seconds when allowed to expand laterally (Fig. 2a). The temperature continued to rise for 60 seconds before reaching a steady value of 37 °C.

3.2. Surface morphology and mechanical properties

SilFoam sponges have a closed-cell cellular structure responsible for their flexibility and high surface area. SEM images of the sponges are shown in Fig. 2(d and e). The porosity was analyzed using ImageJ software. As evident from the images, there is very high porosity, and the pore size distribution is broad. The average porosity of the sponge cross-section is up to 70%. The pore size area distribution was calculated by modeling the pores as ellipses (Fig. 2(d and e)). The distribution shows that most pores lie in the 0 to 10 000 μm^2 range. The hydrophobicity of the sponge surface was studied by contact angle goniometry. As expected from a PDMS substrate, the foam surface is hydrophobic with a contact angle of 111° (Fig. 2(f and g)).[48] The contact angle does not change much after that until the sudden apparent drop. This is due to macropores on the surface, which can adsorb a small quantity of water. This can also increase the surface area of contact with SilFoam with blood, inducing clotting by the aggregation of platelets and clotting factors at the wound.[11] The hydrophobic surface hinders the process of local fluid exchange between wounds and the external environment. This can help prevent contamination of the wound when applied. A hydrophobic surface may also reduce the possibility of secondary bleeding once the dressing is removed.[11,49]

The viscosities of part A and part B were measured to be around 6.5 Pa s and 12.5 Pa s, respectively, low enough for controlled injection through a 50 mL dual barrel syringe by hand (Fig. 3(a)). Interestingly, part B undergoes considerable shear

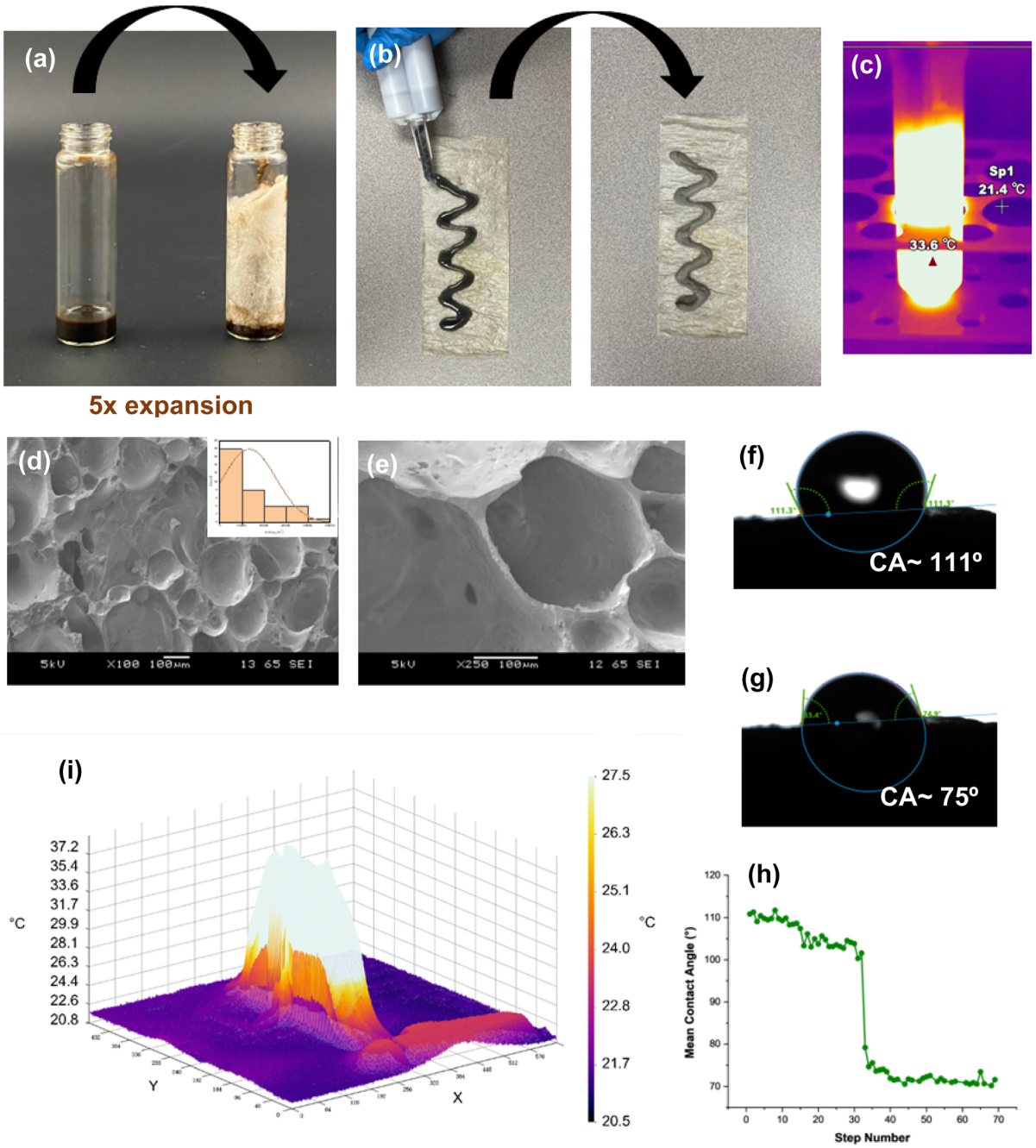

Fig. 2 Fabrication and surface characterization of SilFoam (a) volume expansion of fully crosslinked SilFoam (t = 30 seconds); (b) delivery by a dual-syringe and its expansion; (c) temperature profile during expansion; (d and e) SEM micrographs of porous structure and pore size distribution (inset); (f and g) apparent static water contact angle (CA) on SilFoam surface; (h) apparent contact angle variation with time; (i) spatial heat map of SilFoam expansion.

thinning due to the emulsification of H_2O_2 in the mixture and fumed silica, which was added as a rheological modifier.[50] The rheological behavior of the sponges was analyzed by a time sweep test and axial sweep test, with and without an immersion cup. The crossover point of the storage and loss moduli took place within 5 seconds, denoting the liquid-to-foam point of the hemostatic sponge during application. The storage modulus increases steadily after that before attaining a steady value around the 3 minute mark (Fig. 3(b)). The sponge is almost completely crosslinked around this time. The storage modulus reaches a steady value of around 10 kPa, indicating a very rigid foam. The same experiment was then performed with an immersion cup filled with PBS to simulate blood to study the effect of an aqueous environment on the rheological properties. A very similar trend was observed in this case. The storage modulus values recorded with the PBS were found to

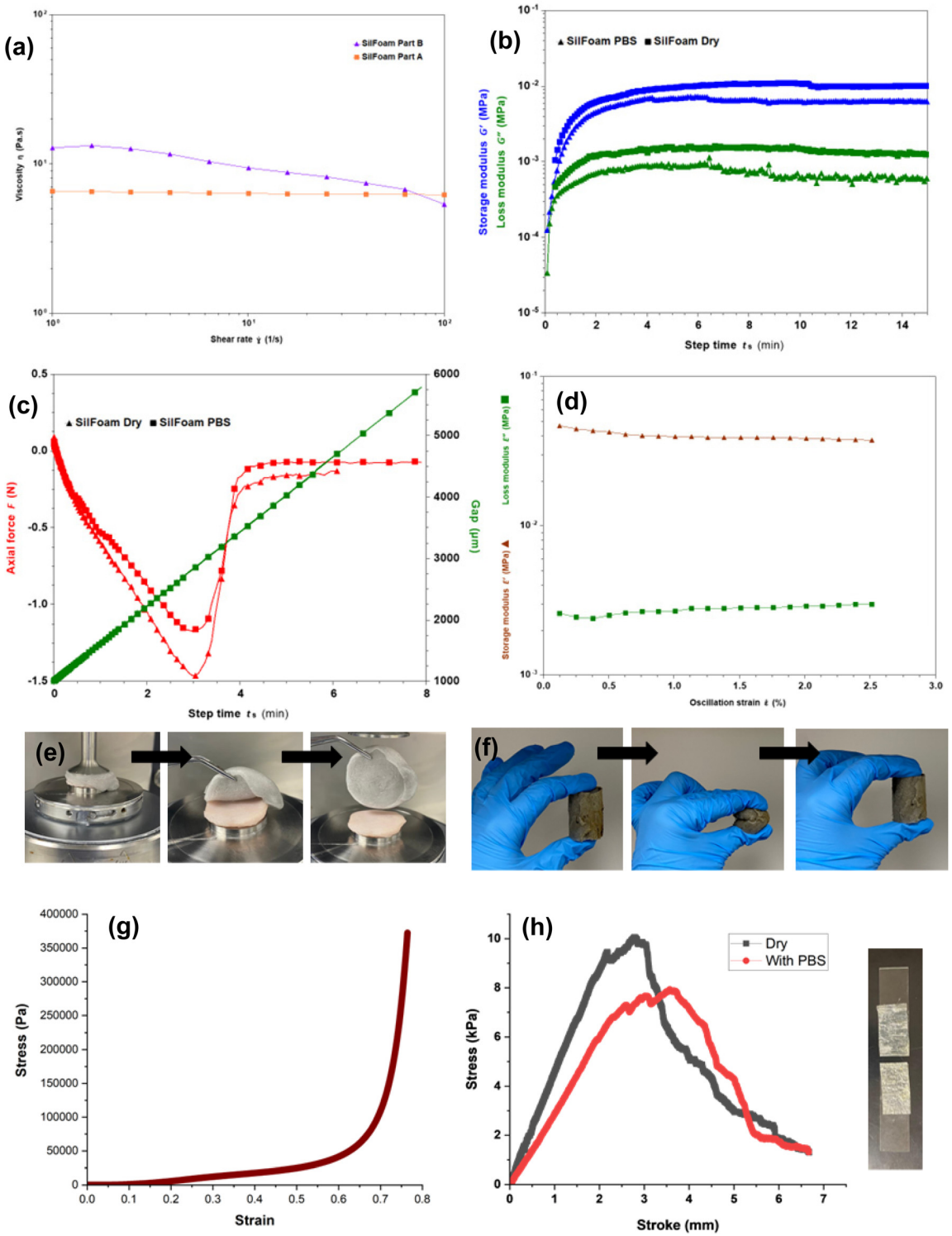

Fig. 3 Mechanical characterization (a) viscosities of SilFoam part A and SilFoam part B; (b) oscillatory time sweep of gel-to-foam reaction; (c) tensile axial test on SilFoam; (d) DMA of cured SilFoam; (e) images showing clean removal of SilFoam post-application on porcine skin; (f) images showing high elasticity and robust structure of SilFoam; (g) compressive stress–strain curve; (h) lap shear tests with sausage skin modified glass slides.

be slightly lower; however, the drop was not significant. The water mixes with the polymer chains, entering the free spaces within and slowing crosslinking. It can also combine with the H_2O_2 in part B, diluting it and lowering the effective reaction rate. Nevertheless, the rigidity of the sponge is not affected significantly by this, and the sponge can expand as usual

(Fig. 3b). Further, axial tests were performed to study the adhesion capability of the sponges. The axial test measures the force required to pull up and detach the head of the plate from the sample after expansion. It was found that a maximum force of around 1.5 N was required for detachment without PBS, which dropped to 1.2 N in the presence of PBS (Fig. 3(c)). It can be concluded that SilFoam can retain its adhesive properties in both dry and wet conditions, making it apt for external and internal wounds, where poor adhesion due to interference from pools of blood is an impediment. The compression strength of SilFoam is high −373 kPa at 70% strain. The compressive modulus is 60 kPa, indicative of a rigid structure (Fig. 3(g)). The DMA of the cured SilFoam sponge shows a storage modulus of 30 kPa (Fig. 3(d)) and expresses a shore hardness value of 6A. The ability to achieve instant adhesion to the wet tissue surfaces is critical for any hemostatic system's success, making SilFoam a promising bandage system with exceptional mechanical integrity. SilFoam was applied to an incision made to a sheet of sausage skin and twisted to assess its ability to stay in place in the presence of torsional forces. It was able to resist heavy twisting but could still be removed seamlessly (ESI Movie 1†).

It is important to note the low lap shear strength (10 kPa dry, 8 kPa wet) (Fig. 3h). In designing surgical adhesives and hemostatic materials, it is typical to emphasize a high lap shear strength to underscore the adhesive capability of the material. This is especially significant for hydrogels and biodegradable or bioresorbable materials, where tissue and cellular attachment are vital.[25,31] However, with SilFoam, we emphasize a strong sealing yet easily removable system due to its capability to expand.

3.3. ATR-FTIR

Fourier Transform Infrared Spectra (FTIR) of SilFoam was collected with a Fast Scan accessory to observe real-time spectra of the sample as part A and part B react. Part A and B FTIR spectra were collected separately before this for reference (ESI Fig. S6†). Part B was loaded onto the detector plate first, followed by adding and mixing part A onto the plate after 30 seconds. The spectrum at t = 10 seconds shows the FTIR spectrum of part B only. Distinctive peaks for PDMS are observed (–CH_3 asymmetric stretching at 2900 cm^{-1}, –CH_3 deformation at 1260 cm^{-1}, Si–O–Si stretching doublet at 1020 cm^{-1}, –CH_3 rocking and Si–C stretching at 790 cm^{-1}), along with broad peaks at around 3440 cm^{-1} and 1650 cm^{-1} due to the presence of dil. H_2O_2.[51] After the addition of part A, significant changes in the spectra are not visible immediately, as over 90% of the sample is PDMS by weight—the attenuation of the peaks corresponding to dil. H_2O_2 with time is of interest, as it is indicative that the H_2O_2 in the sample will diminish as the reaction progresses. Although H_2O is generated as a reaction product, it is not significant enough to manifest itself in the spectrum. At t = 290 seconds, the peaks corresponding to H_2O_2 have diminished almost entirely. There is very little residual H_2O_2 in the system, eliminating any major risk of H_2O_2 leaking into the bloodstream after application and causing venous or intravascular embolism.[52] Nominal concentrations of H_2O_2 on the wound surface may be present, which can promote blood oxygenation and disinfection (Fig. 4).[53]

3.4. Mechanistic hemorrhage manikin model

As biomedical and biotechnological research is booming, so is the demand for *in vivo* models worldwide. However, this comes at a cost. Institutional Review Board (IRB) approvals in the United States can take weeks to months, often an impractical timescale. Similar issues are faced in other parts of the world as well. Pain is another significant issue, specifically in trials where animals are undergoing invasive procedures. In research that involves animal subjects, particularly in surgical trials, the careful selection of anesthesia, analgesic agents, and euthanasia of the subjects after the surgical procedures are crucial. This choice is vital for effectively managing pain related to interventions while ensuring minimal impact on the measured outcomes.[54] Generally, regulatory bodies permit the omission of pain treatment in animal subjects, providing adequate justification.[55] A literature survey has revealed that several animal studies have deliberately refrained from giving procedural analgesia, as it could influence the measured outcomes.[56] Further, concerns are being raised regarding the psychological consequences of performing animal trials and euthanasia. People who work with lab animals can develop perpetration-induced traumatic stress, compassion fatigue, and post-traumatic stress disorder, all of which take a toll on one's mental health. According to a report, nine in ten people in the profession suffer from compassion fatigue at some point in their careers.[57,58] As the design of surgical trials involving animals advances, particular attention must be given to these critical issues, and alternative approaches should be explored whenever feasible.[59,60]

In light of this, SilFoam was tested on a torso hemorrhage model human manikin equipped with an electronic bleeding controller (Fig. 5(a and b)). It is emphasized that while a

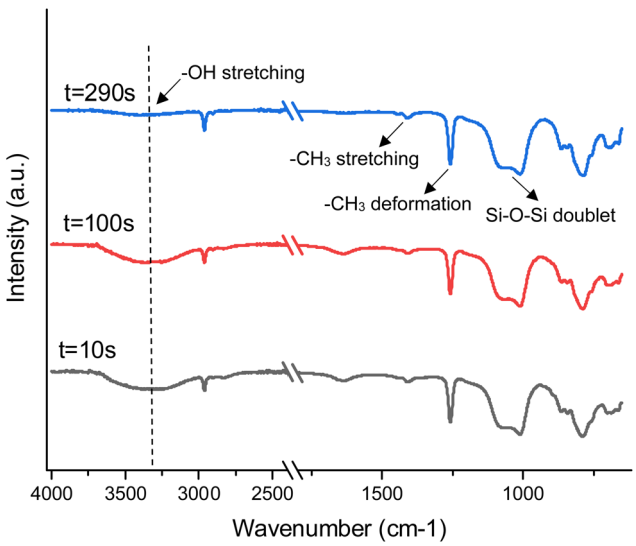

Fig. 4 *In situ* ATR-FTIR of SilFoam formation.

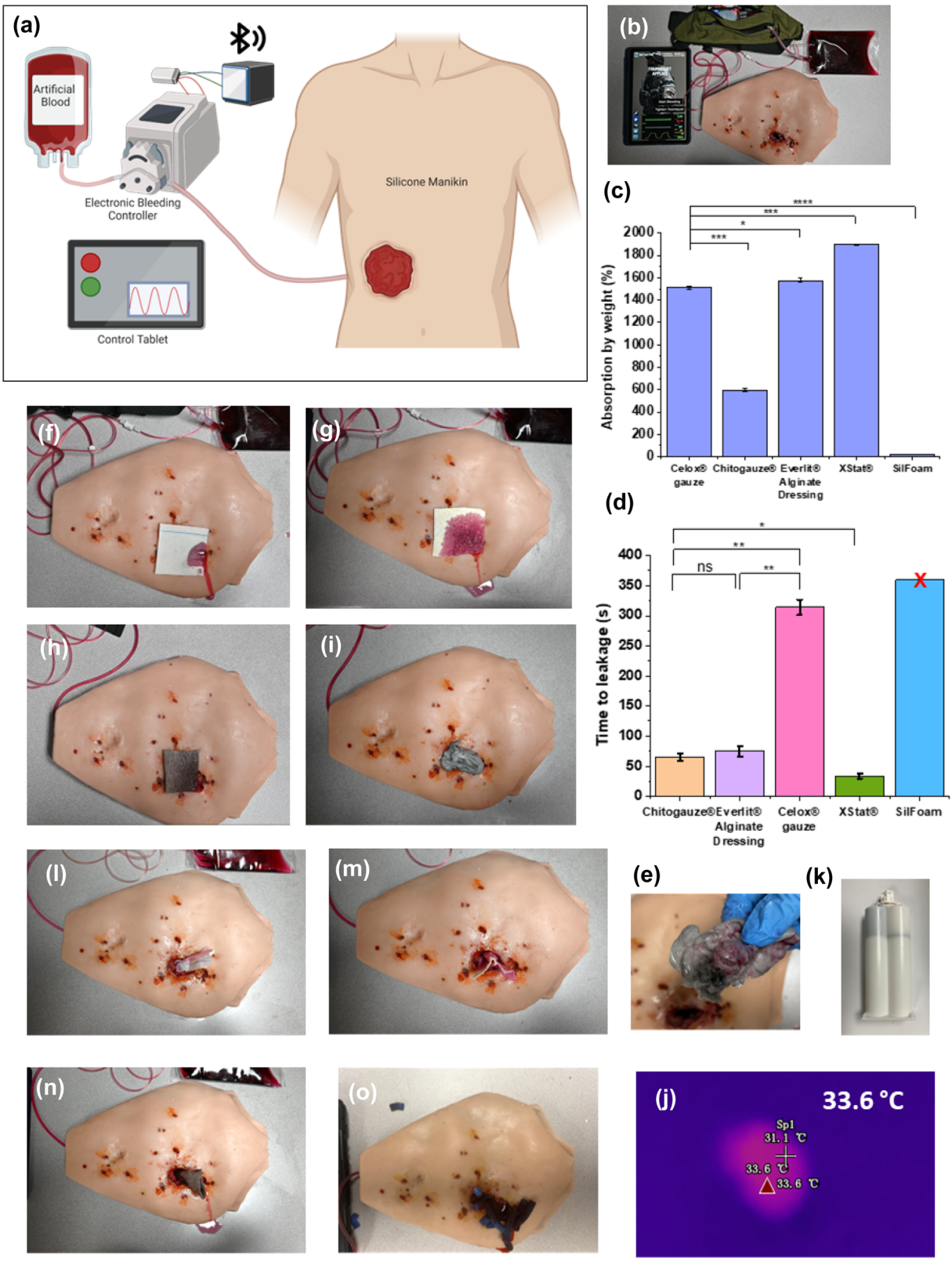

Fig. 5 Mechanistic hemorrhage model testing: (a) simplified scheme of the manikin and electronic bleeding controller; (b) test set-up; (c) fluid absorption by weight of different bandage systems: SilFoam, Celox® gauze, Chitogauze®, XStat®, Everlit® Alginate Dressing; (d) time to leakage of bandage systems: SilFoam, Celox® gauze, Chitogauze®, XStat®, Everlit® Alginate Dressing (x denotes no leakage observed within recorded time); (e) clean removal of SilFoam post application; (f–i) hemostasis testing without wound packing: Chitogauze®, Celox® gauze, Everlit® Alginate Dressing, SilFoam respectively; (j) spatial heat map during SilFoam application; (k) dual-syringe pre-application; (l–o) hemostasis testing with wound packing: Chitogauze®, Celox® gauze, Everlit® Alginate Dressing, XStat®, respectively.

mechanical model such as this cannot replace the significance of *in vivo* assays, it can be a valuable preliminary tool to test relevant materials and provide information about their efficacy from a purely mechanical perspective. Following this model would also enable researchers to select their best formulations for subsequent *in vivo* studies. Since SilFoam is not bioactive but a tamponade-based system, these studies provide valuable insight into its working principle. Popular bandages to arrest heavy bleeding in the field – Celox® gauze, Chitogauze®, XStat®, and Everlit® Alginate Dressing were also tested for comparison. SilFoam effectively stanched a bleeding rate of 0.5 mL per second instantly and did not cause leakage in the time measured (Fig. 5(i)). During application, an IR gun was used to read the temperature of the reacting SilFoam, and a maximum temperature of 33.6 °C was measured (Fig. 5(j)). Without manual pressure and wound packing, all the tested hemostatic bandages led to leakage within 30 seconds (Fig. 5 (f–h)). With packing, Chitogauze® led to leakage in 60 seconds, Everlit® Alginate Dressing led to leakage in 75 seconds, and XStat® in 35 seconds, while Celox® gauze held out for up to 300 seconds without leakage (Fig. 5(l–o)). However, Celox® gauze was seen to absorb up to 1530% of its weight, Everlit® Alginate Dressing up to 1560% of its weight, XStat® up to 1890%, and Chitogauze® up to 600% of its weight in artificial blood (Fig. 5(c)). Hence, although they can prevent leakage, they are ineffective at preventing blood loss altogether. While swelling and absorption can aid clotting and wound healing in the presence of bioactive substances by improving blood–material interaction, in emergencies where uncontrollable bleeding poses high fatality risks, it is imperative that bleeding is controlled as soon as possible by any means. The autogenous pressure generated by the rapidly expanding SilFoam at the wound site aids it in forming an effective seal that conforms to and around the wound with minimal fluid absorption. SilFoam was found to absorb only up to 20% of its weight in artificial blood due to its hydrophobic nature and closed-cell structure, preventing unnecessary blood loss and enabling its effectiveness even in adverse weather conditions such as rain. The good injectability suggests that SilFoam could potentially be applied to narrow and deep wounds, as the subsequent rapid volume expansion would allow it to fill irregular wound boundaries with different shapes perfectly. SilFoam could also withstand a higher flow rate of 0.7 mL per second (ESI Fig. S9†) without any signs of leakage (ESI Movie 2† shows the application of SilFoam on the manikin). Further, it can be removed cleanly without leaving any residue (Fig. 5(e), ESI Movie 3†). It was also observed that XStat®, a commercial hemostatic agent with a similar mechanical working principle, was exceedingly cumbersome to remove due to the presence of multiple compressed sponges injected into the wound and is likely to inflict unwanted pain to the patient. In comparison, SilFoam provides a more robust seal following a tamponade principle and is easily removable in one piece. It should be noted here that Celox®, Chitogauze®, and Everlit® Alginate Dressing possess bioactive components that aid blood clotting, which are not considered here. This experiment characterizes the sealing capacity of these gauzes in the absence of manual compression.

3.5. Biocompatibility studies and antibacterial assays

The Minimal Essential Media (MEM) Elution test was designed to determine the cytotoxicity of extractable substances. An extract of cured SilFoam was added to cell monolayers and incubated. The cell monolayers were examined and scored based on the degree of cellular destruction. The United States Pharmacopeia & National Formulary (USP) states that the test article receives a passing score if the reactivity grade is not greater than grade 2 or has a mild reactivity. The ANSI/AAMI/ISO 10993-5 standard states that achieving a numerical grade greater than 2 is a cytotoxic effect. The acceptance criteria were based on the negative and media controls receiving "0" reactivity grades and positive controls receiving a 3–4 reactivity grade (moderate to severe).

SilFoam passed the qualitative MEM Elution cytotoxicity test (Table 1). The solution was clear with no particulates or color changes, pre- and post-extraction. A leaching test for silver ions was performed to quantify the release of silver ions into the bloodstream, assessing the potential cytotoxicity associated with their presence. The concentration of silver ions in solution 1 hour and 24 hours post immersion was <1 ppm from ICP-OES analyses. The quantitative cytotoxicity test (MTT) was done to determine the biological reactivity of SilFoam and involved exposing an extract of SilFoam to L929 mouse fibroblast cells. The cells were allowed to grow in the presence of the extracted fluid before adding a tetrazolium

Table 1 MEM elution cytotoxicity test

Identification	Results (pass/fail)	Scores #1	#2	#3	Average	Extraction ratio
SilFoam	Pass	2	2	2	2	0.2 g mL^{-1}
Polypropylene pellets	Pass	0	0	0	0	0.2 g mL^{-1}
Latex natural rubber	Fail	4	4	4	4	0.2 g mL^{-1}

Table 2 MTT assay cytotoxicity test

SilFoam extract condition	Mean percent viability
2-Fold diluted (50%)	71
4-Fold diluted (25%)	77
8-Fold diluted (12.5%)	82

Table 3 Hemolytic index

Test article	Average optical density	Hemolytic index (%)
SilFoam	0.005	0.82
Negative control (polypropylene pellets)	0.001	0.00
Positive control (nitrile glove)	0.363	89.3
PBS blank	0.002	N/A

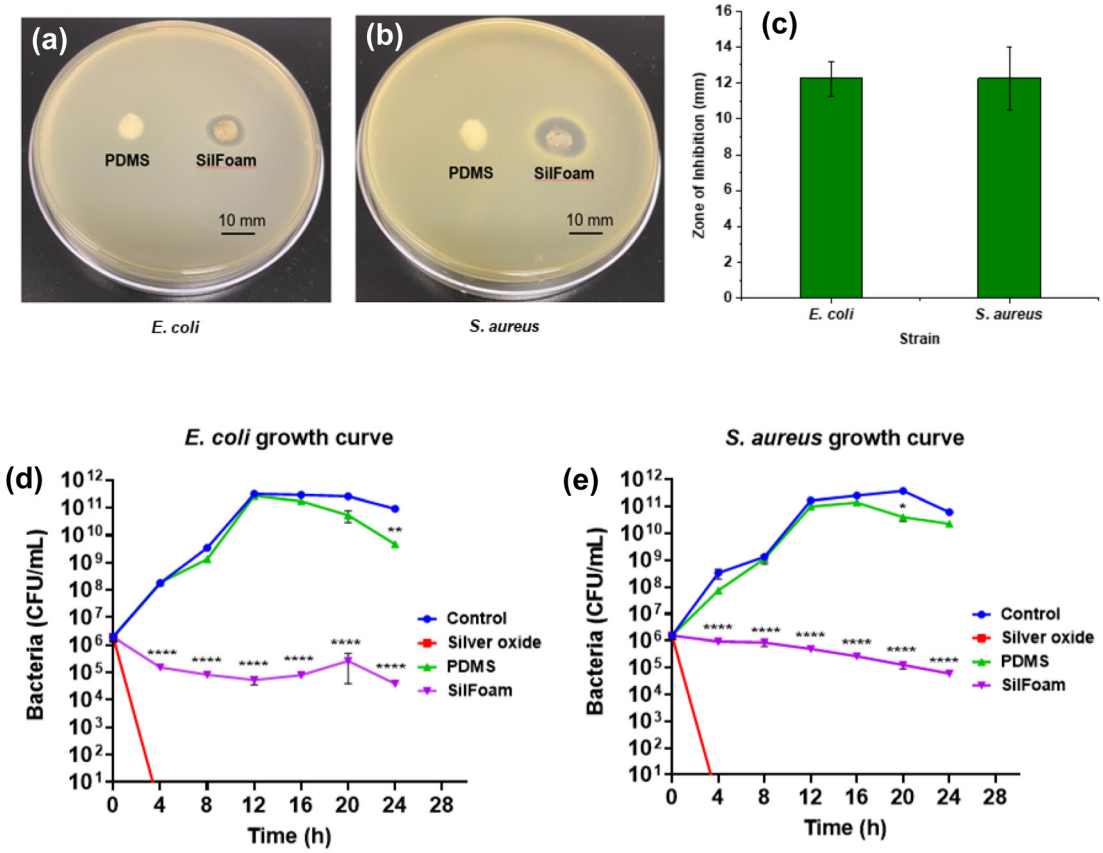

Fig. 6 (a and b) Antibacterial activity against *S. aureus* and *E. coli*, respectively; (c) zones of inhibition; (d) *E. coli* growth curve; (e) *S. aureus* growth curve.

dye (MTT), which was used to assess the metabolic activity of cultures. MTT (3-(4,5-dimethylthiazol-2-yl)-2,5-diphenyltetrazolium bromide) is a yellow dye that turns purple when metabolized by viable cells. The number of viable cells correlates to the degree of color change when measured on a spectrophotometer at 570 nm. The results are reported as percent viability (% living cells), where cell viability ≥70% indicates the sample does not have a cytotoxic potential. SilFoam indicated no cytotoxic potential (Table 2). Further, SilFoam was found to express a hemolytic index of only 0.82% after a 24 hour extraction period, suggesting it has no hemolytic potential, as shown in Table 3 (hemolytic index 0–2: non-hemolytic; 2–5: slightly hemolytic; >5: hemolytic).

Disc diffusion assays for testing the antibacterial effect of SilFoam have shown that SilFoam is effective against both Gram-positive (*S. aureus*) and Gram-negative (*E. coli*) strains of bacteria (Fig. 6(a–c)). The growth curves of *E. coli* and *S. aureus* further corroborate this, and it is evident that Ag_2O is responsible for the antibacterial activity observed (Fig. 6(d and e)). The colonies 24 hours post-incubation can be seen in ESI Fig. S9.† This can be attributed to the well-established antibacterial effect of Ag_2O present. Silver-based compounds are known to cause bacterial death by several strategies, such as disturbing the permeability of bacterial membranes, inactivating proteins, hindering DNA replication, and interacting with respiratory enzymes. It has been shown that silver can accumulate in microorganisms as Ag^0, Ag_2O, and Ag^+, which are all responsible for the bactericidal strategies mentioned above.[61] Further, some researchers have shown the synergistic effect of Ag and H_2O_2 on antimicrobial efficacy, which could also be at play here.[46]

4. Conclusion

In summary, SilFoam, a rapid-action hemostat with antimicrobial properties, has been developed, showing immense promise in trauma management and prehospital care. The hassle-free delivery and rapid action make it a versatile treatment to stop heavy bleeding, while its hydrophobic nature also allows it to be used in inclement weather conditions. The mechanical properties have been optimized for use by victims of civilian trauma and soldiers on active duty. Its excellent injectability suggests that SilFoam could be applied to irregular wounds, and the rapid curing and expansion allow it to penetrate and conform around irregularly shaped wounds and crevices. Further, SilFoam displays antibacterial capabilities against Gram-positive and Gram-negative bacterial strains.

This study was focused on evaluating the tamponade capabilities of SilFoam using a mechanistic hemorrhage model, which allows the circumvention of time-consuming and costly *in vivo* models for initial screening and testing. Unlike many other hemostatic products currently available, SilFoam is mechanically durable, hydrophobic, and very easy to remove. The comparison studies have shown SilFoam to outperform all the different commercial products tested, including XStat®, which follows a similar mechanism of action but has proved very difficult to remove from the wound site. It is anticipated that SilFoam can be used successfully to tackle bleeding, both from open wounds and internal bleeding, for which coagulopathy and non-coagulopathy injury models will be employed soon. Consequently, the optimized SilFoam will be tested on *in vivo* models for a more holistic evaluation of its effectiveness.

Author contributions

P. Sarkar: Conceptualization, methodology, formal analysis, investigation, writing – original draft, review & editing. A. Pugazhendhi: Antimicrobial assays – methodology, formal analysis, investigation, writing – original draft, review & editing. M. Coathup: Antimicrobial assays – resources, supervision, writing – review & editing. K. Mukhopadhyay: Conceptualization, resources, writing – original draft, review & editing, supervision, project administration, funding acquisition.

Conflicts of interest

The authors declare that they have no known competing financial interests reported in this paper. UCF has filed a US Patent application on this work on behalf of the authors (P. S. and K. M.).

Acknowledgements

This work was partially supported by a startup fund and the GAP fund from UCF for Dr K. Mukhopadhyay. We acknowledge the Doctoral Fellowship for P. S. awarded by the UCF Board of Trustees; UCF Materials Characterization Facility (MCF) for characterization; Angela Alban and Daniel Webster from SIMETRI, Inc. for kindly providing the torso hemorrhage model (manikin) for testing; Galbraith Laboratories (Knoxville, Tennessee, USA) for ICP-OES characterization support on pay-per-use basis; Nelson Labs (Salt Lake City, USA) for cytotoxicity and hemolysis characterization support on pay-per-use basis; Evonik Inc. for kindly providing the fumed silica used in this study. All chemical structures and figures were made using Biorender.com.

References

1 D. Johnson, S. Bates, S. Nukalo, A. Staub, A. Hines, T. Leishman, J. Michel, D. Sikes, B. Gegel and J. Burgert, The Effects of QuikClot Combat Gauze on Hemorrhage Control in the Presence of Hemodilution and Hypothermia, *Ann. Med. Surg.*, 2014, **3**(2), 21–25, DOI: **10.1016/j.amsu.2014.03.001**.

2 D. Hee Park, S. Bum Kim, K.-D. Ahn, E. Yong Kim, Y. Jun Kim and D. Keun Han, In Vitro Degradation and Cytotoxicity of Alkyl 2-Cyanoacrylate Polymers for Application to Tissue Adhesives, *J. Appl. Polym. Sci.*, 2003, **89**(12), 3272–3278, DOI: **10.1002/app.12452**.

3 J. Wen, M. Weinhart, B. Lai, J. Kizhakkedathu and D. E. Brooks, Reversible Hemostatic Properties of Sulfabetaine/Quaternary Ammonium Modified Hyperbranched Polyglycerol, *Biomaterials*, 2016, **86**, 42–55, DOI: **10.1016/j.biomaterials.2016.01.067**.

4 A. M. Behrens, M. J. Sikorski and P. Kofinas, Hemostatic Strategies for Traumatic and Surgical Bleeding, *J. Biomed. Mater. Res., Part A*, 2014, **102**(11), 4182–4194, DOI: **10.1002/jbm.a.35052**.

5 U. Katzenell, N. Ash, A. L. Tapia, G. A. Campino and E. Glassberg, Analysis of the Causes of Death of Casualties in Field Military Setting, *Mil. Med.*, 2012, **177**(9), 1065–1068, DOI: **10.7205/MILMED-D-12-00161**.

6 J. A. Chambers, K. Seastedt, R. Krell, E. Caterson, M. Levy and N. Turner, "Stop the Bleed": A U.S. Military Installation's Model for Implementation of a Rapid Hemorrhage Control Program, *Mil. Med.*, 2019, **184**(3–4), 67–71, DOI: **10.1093/milmed/usy185**.

7 H. Carmichael, L. Steward, E. D. Peltz, F. L. Wright and C. G. Velopulos, Preventable Death and Interpersonal Violence in the United States: Who Can Be Saved?, *J. Trauma Acute Care Surg.*, 2019, **87**(1), 200, DOI: **10.1097/TA.0000000000002336**.

8 Z. Chen, L. Han, C. Liu, Y. Du, X. Hu, G. Du, C. Shan, K. Yang, C. Wang, M. Li, F. Li and F. Tian, A Rapid Hemostatic Sponge Based on Large, Mesoporous Silica Nanoparticles and N-Alkylated Chitosan, *Nanoscale*, 2018, **10**(43), 20234–20245, DOI: **10.1039/C8NR07865C**.

9 H. Montazerian, E. Davoodi, A. Baidya, S. Baghdasarian, E. Sarikhani, C. E. Meyer, R. Haghniaz, M. Badv, N. Annabi, A. Khademhosseini and P. S. Weiss, Engineered Hemostatic Biomaterials for Sealing Wounds, *Chem. Rev.*, 2022, **122**(15), 12864–12903, DOI: **10.1021/acs.chemrev.1c01015**.

10 Z.-Y. Zhang, H.-Y. Zhang, T. Talmy, Y. Guo, S.-R. Zhou, L.-Y. Zhang and Y. Li, Management of Non-Compressible Torso Hemorrhage: An Update, *Chin. J. Traumatol.*, 2021, **24**(3), 125–131, DOI: **10.1016/j.cjtee.2021.03.005**.

11 Y. Guo, M. Wang, Q. Liu, G. Liu, S. Wang and J. Li, Recent Advances in the Medical Applications of Hemostatic Materials, *Theranostics*, 2023, **13**(1), 161–196, DOI: **10.7150/thno.79639**.

12 X. Liao, M. Guo, J. Wen, W. Huang, H. Ye and B. Li, Pulmonary Embolism Caused by Tourniquets in the Lower Extremities Treated with ECMO – A Case Report, *Heart Surg. Forum*, 2022, **25**(3), E449–E451, DOI: **10.1532/hsf.4635**.

13 Z. Yang, L. Chen, J. Liu, H. Zhuang, W. Lin, C. Li and X. Zhao, Short Peptide Nanofiber Biomaterials Ameliorate Local Hemostatic Capacity of Surgical Materials and Intraoperative Hemostatic Applications in Clinics, *Adv. Mater.*, 2023, **35**(39), 2301849, DOI: **10.1002/adma.202301849**.

14 S. Ghimire, P. Sarkar, K. Rigby, A. Maan, S. Mukherjee, K. E. Crawford and K. Mukhopadhyay, Polymeric Materials for Hemostatic Wound Healing, *Pharmaceutics*, 2021, **13**(12), 2127, DOI: **10.3390/pharmaceutics13122127**.

15 S. Pourshahrestani, E. Zeimaran, N. A. Kadri, N. Mutlu and A. R. Boccaccini, Polymeric Hydrogel Systems as Emerging Biomaterial Platforms to Enable Hemostasis and Wound Healing, *Adv. Healthcare Mater.*, 2020, **9**(20), 2000905, DOI: **10.1002/adhm.202000905**.

16 C. C. Cloonan, Treating Traumatic Bleeding in a Combat Setting, *Mil. Med.*, 2004, **169**(suppl_12), 8–10, DOI: **10.7205/MILMED.169.12S.8**.

17 S. Jiao, X. Zhang, H. Cai, S. Wu, X. Ou, G. Han, J. Zhao, Y. Li, W. Guo, T. Liu and W. Qu, Recent Advances in Biomimetic Hemostatic Materials, *Mater. Today Bio*, 2023, **19**, 100592, DOI: **10.1016/j.mtbio.2023.100592**.

18 P. Nakielski and F. Pierini, Blood Interactions with Nano- and Microfibers: Recent Advances, Challenges and Applications in Nano- and Microfibrous Hemostatic Agents, *Acta Biomater.*, 2019, **84**, 63–76, DOI: **10.1016/j.actbio.2018.11.029**.

19 L. E. Stuke, Prehospital Topical Hemostatic Agents – A Review of the Current Literature.

20 L. Bedford, *The Case Against QuikClot*. The Survival Mom. **https://thesurvivalmom.com/the-case-against-quikclot/** (accessed 2023-10-26).

21 J. Varshosaz, The Promise of Chitosan Microspheres in Drug Delivery Systems, *Expert Opin. Drug Delivery*, 2007, **4**(3), 263–273, DOI: **10.1517/17425247.4.3.263**.

22 Y. Xia, R. Yang, H. Wang, Y. Li and C. Fu, Application of Chitosan-Based Materials in Surgical or Postoperative Hemostasis, *Front. Mater.*, 2022, **9**, 1–9.

23 D. A. Liening, L. Lundy, B. Silberberg and K. Finstuen, A Comparison of the Biocompatibility of Three Absorbable Hemostatic Agents in the Rat Middle Ear, *Otolaryngol.–Head Neck Surg.*, 1997, **116**(4), 454–457, DOI: **10.1016/S0194-59989770294-8**.

24 K. Zheng, Q. Gu, D. Zhou, M. Zhou and L. Zhang, Recent Progress in Surgical Adhesives for Biomedical Applications, *Smart Mater. Med.*, 2022, **3**, 41–65, DOI: **10.1016/j.smaim.2021.11.004**.

25 Y. Hong, F. Zhou, Y. Hua, X. Zhang, C. Ni, D. Pan, Y. Zhang, D. Jiang, L. Yang, Q. Lin, Y. Zou, D. Yu, D. E. Arnot, X. Zou, L. Zhu, S. Zhang and H. Ouyang, A Strongly Adhesive Hemostatic Hydrogel for the Repair of Arterial and Heart Bleeds, *Nat. Commun.*, 2019, **10**(1), 2060, DOI: **10.1038/s41467-019-10004-7**.

26 Y. Ouyang, Y. Zhao, X. Zheng, Y. Zhang, J. Zhao, S. Wang and Y. Gu, Rapidly Degrading and Mussel-Inspired Multifunctional Carboxymethyl Chitosan/Montmorillonite Hydrogel for Wound Hemostasis, *Int. J. Biol. Macromol.*, 2023, **242**, 124960, DOI: **10.1016/j.ijbiomac.2023.124960**.

27 J. Su, J. Li, J. Liang, K. Zhang and J. Li, Hydrogel Preparation Methods and Biomaterials for Wound Dressing, *Life*, 2021, **11**(10), 1016, DOI: **10.3390/life11101016**.

28 M. Liang, D. Wei, Z. Yao, P. Ren, J. Dai, L. Xu, T. Zhang and Q. Zhang, Hydrogel Adhesive Formed via Multiple Chemical Interactions: From Persistent Wet Adhesion to Rapid Hemostasis, *Biomater. Sci.*, 2022, **10**(6), 1486–1497, DOI: **10.1039/D1BM01848E**.

29 X. Du, L. Wu, H. Yan, Z. Jiang, S. Li, W. Li, Y. Bai, H. Wang, Z. Cheng, D. Kong, L. Wang and M. Zhu, Microchannelled Alkylated Chitosan Sponge to Treat Noncompressible Hemorrhages and Facilitate Wound Healing, *Nat. Commun.*, 2021, **12**(1), 4733, DOI: **10.1038/s41467-021-24972-2**.

30 A. Nepal, H. D. N. Tran, N.-T. Nguyen and H. T. Ta, Advances in Haemostatic Sponges: Characteristics and the Underlying Mechanisms for Rapid Haemostasis, *Bioact. Mater.*, 2023, **27**, 231–256, DOI: **10.1016/j.bioactmat.2023.04.008**.

31 N. Annabi, Y.-N. Zhang, A. Assmann, E. S. Sani, G. Cheng, A. D. Lassaletta, A. Vegh, B. Dehghani, G. U. Ruiz-Esparza, X. Wang, S. Gangadharan, A. S. Weiss and A. Khademhosseini, Engineering a Highly Elastic Human Protein–Based Sealant for Surgical Applications, *Sci. Transl. Med.*, 2017, **9**(410), eaai7466, DOI: **10.1126/scitranslmed.aai7466**.

32 H. T. Beaman, E. Shepherd, J. Satalin, S. Blair, H. Ramcharran, S. Serinelli, L. Gitto, K. S. Dong, D. Fikhman, G. Nieman, S. G. Schauer and M. B. B. Monroe, Hemostatic Shape Memory Polymer Foams with Improved Survival in a Lethal Traumatic Hemorrhage Model, *Acta Biomater.*, 2022, **137**, 112–123, DOI: **10.1016/j.actbio.2021.10.005**.

33 Y. He, J. Wang, Y. Si, X. Wang, H. Deng, Z. Sheng, Y. Li, J. Liu and J. Zhao, A Novel Gene Recombinant Collagen Hemostatic Sponge with Excellent Biocompatibility and Hemostatic Effect, *Int. J. Biol. Macromol.*, 2021, **178**, 296–305, DOI: **10.1016/j.ijbiomac.2021.02.162**.

34 K. Quan, G. Li, D. Luan, Q. Yuan, L. Tao and X. Wang, Black Hemostatic Sponge Based on Facile Prepared Cross-Linked Graphene, *Colloids Surf., B*, 2015, **132**, 27–33, DOI: **10.1016/j.colsurfb.2015.04.067**.

35 J. Chen, L. Lv, Y. Li, X. Ren, H. Luo, Y. Gao, H. Yan, Y. Li, Y. Qu, L. Yang, X. Li and R. Zeng, Preparation and Evaluation of Bletilla Striata Polysaccharide/Graphene Oxide Composite Hemostatic Sponge, *Int. J. Biol. Macromol.*, 2019, **130**, 827–835, DOI: **10.1016/j.ijbiomac.2019.02.137**.

36 L. Zheng, Q. Wang, Y. S. Zhang, H. Zhang, Y. Tang, Y. Zhang, W. Zhang and X. Zhang, A Hemostatic Sponge Derived from Skin Secretion of Andrias Davidianus and Nanocellulose, *Chem. Eng. J.*, 2021, **416**, 129136, DOI: **10.1016/j.cej.2021.129136**.

37 H. Choudhary, M. B. Rudy, M. B. Dowling and S. R. Raghavan, Foams with Enhanced Rheology for

Stopping Bleeding, *ACS Appl. Mater. Interfaces*, 2021, **13**(12), 13958–13967, DOI: **10.1021/acsami.0c22818**.

38 J. C. Chang, B. C. Holloway, M. Zamisch, M. J. Hepburn and G. S. F. Ling, ResQFoam for the Treatment of Non-Compressible Hemorrhage on the Front Line, *Mil. Med.*, 2015, **180**(9), 932–933, DOI: **10.7205/MILMED-D-15-00049**.

39 L. Yu and A. L. Skov, Monolithic Growth of Partly Cured Polydimethylsiloxane Thin Film Layers, *Polym. J.*, 2014, **46**(2), 123–129, DOI: **10.1038/pj.2013.72**.

40 A. G. Bejenariu, L. Yu and A. L. Skov, Low Moduli Elastomers with Low Viscous Dissipation, *Soft Matter*, 2012, **8**(14), 3917, DOI: **10.1039/c2sm25134e**.

41 H. H. Winter and F. Chambon, Analysis of Linear Viscoelasticity of a Crosslinking Polymer at the Gel Point, *J. Rheol.*, 1986, **30**(2), 367–382, DOI: **10.1122/1.549853**.

42 P.-C. Lin, S. Vajpayee, A. Jagota, C.-Y. Hui and S. Yang, Mechanically Tunable Dry Adhesive from Wrinkled Elastomers, *Soft Matter*, 2008, **4**(9), 1830–1835, DOI: **10.1039/B802848F**.

43 S. Suvarnapathaki, X. Wu, D. Lantigua, M. A. Nguyen and G. Camci-Unal, Breathing Life into Engineered Tissues Using Oxygen-Releasing Biomaterials, *NPG Asia Mater.*, 2019, **11**(1), 1–18, DOI: **10.1038/s41427-019-0166-2**.

44 S. Petlitckaia and A. Poulesquen, Design of Lightweight Metakaolin Based Geopolymer Foamed with Hydrogen Peroxide, *Ceram. Int.*, 2019, **45**(1), 1322–1330, DOI: **10.1016/j.ceramint.2018.10.021**.

45 C. Sturgess, C. Tuck, I. Ashcroft and R. Wildman, 3D Reactive Inkjet Printing of Polydimethylsiloxane, *J. Mater. Chem. C*, 2017, **5**, 9733–9743, DOI: **10.1039/C7TC02412F**.

46 M. Y. Alkawareek, A. Bahlool, S. R. Abulateefeh and A. M. Alkilany, Synergistic Antibacterial Activity of Silver Nanoparticles and Hydrogen Peroxide, *PLoS One*, 2019, **14**(8), e0220575, DOI: **10.1371/journal.pone.0220575**.

47 B. B. Ong and N. Milne, Injury, Fatal and Nonfatal: Burns and Scalds, in *Encyclopedia of Forensic and Legal Medicine*, ed. J. Payne-James and R. W. Byard, Elsevier, Oxford, 2nd edn, 2016, pp. 173–181. DOI: **10.1016/B978-0-12-800034-2.00220-2**.

48 T. Trantidou, Y. Elani, E. Parsons and O. Ces, Hydrophilic Surface Modification of PDMS for Droplet Microfluidics Using a Simple, Quick, and Robust Method via PVA Deposition, *Microsyst. Nanoeng.*, 2017, **3**(1), 1–9, DOI: **10.1038/micronano.2016.91**.

49 Z. Li, A. Milionis, Y. Zheng, M. Yee, L. Codispoti, F. Tan, D. Poulikakos and C. H. Yap, Superhydrophobic Hemostatic Nanofiber Composites for Fast Clotting and Minimal Adhesion, *Nat. Commun.*, 2019, **10**(1), 5562, DOI: **10.1038/s41467-019-13512-8**.

50 P. Sarkar, S. Ghimire, S. Vlasov and K. Mukhopadhyay, Effect of Clay-Zwitterionic Interactions in Controlling the Viscoelastic Properties in Organomodified Clays, *iScience*, 2023, **26**(12), 108388, DOI: **10.1016/j.isci.2023.108388**.

51 J. Lee, J. Kim, H. Kim, Y. M. Bae, K.-H. Lee and H. J. Cho, Effect of Thermal Treatment on the Chemical Resistance of Polydimethylsiloxane for Microfluidic Devices, *J. Micromech. Microeng.*, 2013, **23**(3), 035007, DOI: **10.1088/0960-1317/23/3/035007**.

52 J. M. DiBianco, J. Lange, D. Heidenberg and P. Mufarrij, Oxygen Venous Embolism After Hydrogen Peroxide Use During Percutaneous Nephrolithotomy, *J. Endourol. Case Rep.*, 2019, **5**(1), 25–27, DOI: **10.1089/cren.2018.0111**.

53 G. Zhu, Q. Wang, S. Lu and Y. Niu, Hydrogen Peroxide: A Potential Wound Therapeutic Target?, *Med. Princ. Pract.*, 2017, **26**(4), 301–308, DOI: **10.1159/000475501**.

54 L. Carbone and J. Austin, Pain and Laboratory Animals: Publication Practices for Better Data Reproducibility and Better Animal Welfare, *PLoS One*, 2016, **11**(5), e0155001, DOI: **10.1371/journal.pone.0155001**.

55 National Research Council (US) Committee for the Update of the Guide for theCare and Use of Laboratory Animals. *Guide for the Care and Use of Laboratory Animals*, The National Academies Collection: Reports funded by National Institutes of Health; National Academies Press (US), Washington (DC), 8th edn, 2011.

56 L. Carbone, Pain in Laboratory Animals: The Ethical and Regulatory Imperatives, *PLoS One*, 2011, **6**(9), e21578, DOI: **10.1371/journal.pone.0021578**.

57 Suffering in silence: Caring for research animals can take a severe mental toll. **https://www.science.org/content/article/suffering-silence-caring-research-animals-can-take-severe-mental-toll** (accessed 2024-04-11).

58 K. Cooney and B. Kipperman, Ethical and Practical Considerations Associated with Companion Animal Euthanasia, *Animals*, 2023, **13**(3), 430, DOI: **10.3390/ani13030430**.

59 K. Taylor, *Reporting the Implementation of the Three Rs in European Primate and Mouse Research Papers: Are We Making Progress?*, 2010.

60 N. B. Robinson, K. Krieger, F. M. Khan, W. Huffman, M. Chang, A. Naik, R. Yongle, I. Hameed, K. Krieger, L. N. Girardi and M. Gaudino, The Current State of Animal Models in Research: A Review, *Int. J. Surg.*, 2019, **72**, 9–13, DOI: **10.1016/j.ijsu.2019.10.015**.

61 Z. Xu, C. Zhang, X. Wang and D. Liu, Release Strategies of Silver Ions from Materials for Bacterial Killing, *ACS Appl. Bio Mater.*, 2021, **4**(5), 3985–3999, DOI: **10.1021/acsabm.0c01485**.